Journal of Controlled Release 131 (2008) 205–210

Contents lists available at ScienceDirect

Journal of Controlled Release

journal homepage: www.elsevier.com/locate/jconrel

Experimental study on cell self-sealing during sonoporation

Fang Yang [a], Ning Gu [a,*], Di Chen [b], Xiaoyu Xi [c], Dong Zhang [c], Yixin Li [a], Junru Wu [b]

[a] Jiangsu Laboratory for Biomaterials and Devices, State Key Laboratory of Bioelectronics, School of Biological Science and Medical Engineering, Southeast University, Nanjing, 210096, China
[b] Department of Physics, University of Vermont, Burlington, VT 05405, USA
[c] Institute of Acoustics, Nanjing University, Nanjing, 210093, China

ARTICLE INFO

Article history:
Received 12 May 2008
Accepted 26 July 2008
Available online 5 August 2008

Keywords:
Sonoporation
Self-sealing
Cell viability
Drug delivery
LAMP-1

ABSTRACT

Reparable sonoporation of human breast cancer cells was achieved during exposure to moderate ultrasound (spatial peak acoustic pressure, p_{sp}=0.25 MPa, 1 MHz tone-bursts, 20 cycles per tone-burst at pulse repetition frequency of 10 kHz) up to 40 s assisted by the presence of encapsulated microbubbles (EMBs). It was demonstrated that shear stress generated by oscillating EMBs at the cell membranes introduced small transient pores in cell membranes by which cells were able to uptake some extracellular fluid and meanwhile triggered the repairing process through self-sealing during sonoporation. It was also indicated by post-sonoporation analysis using the fluorescent microscopy, scanning electron microscopy, and the Bradford assay which determined the protein content in cell supernatant that the self-sealing might be established by lysosomal-associated membrane protein, LAMP-1, fusing with the plasma membrane under the stressful condition in sonoporation.

1. Introduction

It has been reported [1–10] that oscillating encapsulated microbubbles (EMBs) excited by moderate ultrasound (US) could make cell membranes of nearby cells temporarily 'open' letting macromolecules be delivered into cells. The process usually is a transient phenomenon; the cells can reseal themselves and still keep their vitality after sonication. This technique is called reparable sonoporation [11]. Reparable sonoporation has the potential to be a non-viral transfection tool to deliver DNA or drug safely and efficiently into a cell [12,13], because it has a unique niche such as site specificity (US can be easily focused into a desired volume) and ease of manipulating parameters of US for applications *in vivo*. Several groups of researchers [14–18,19] have tried to understand the possible mechanisms of the reparable sonoporation. Their results have suggested that the possible candidates may include (1) EMBs excited by US promote endocytosis, a process by which a cell uptakes some of its extracellular fluid including material dissolved or suspended in it through its endogenous cellular machinery, e.g., surface receptor sites such as caveoli; (2) shear stress produced by the interaction among cells and oscillating EMBs generates transient, nanometer size pores in plasma membranes through which macromolecules may get inside of cells [17,20].

It is known that when cell membranes suffer emergent disruption, 'resealing' process may be triggered. 'Resealing' is a complex and dynamic cell adaption process which is needed for cell survival [21–23]. It has been reported that cell membrane disruption may trigger Ca^{2+} entering the disruption area and cause vesicles to present in cytoplasm underlying the disruption site to fuse rapidly with one another and also with the adjacent plasma membrane [21,24]. Lysosomes, membrane-bound organelles, have been recognized to play an important role in repairing of plasma membrane 'wounds' [21]. It was also found that LAMP-1, a lysosomal-associated membrane protein, normally is not presented at the plasma membrane surface, became ubiquitously exposed on the cell surface [21,22] when lysosomes were triggered to fuse with the plasma membrane under stressful condition. Up to the authors' knowledge, there is no publication which has addressed the question whether the similar process occurs during the reparable sonoporation; i.e., the shear stress generated by the oscillating EMBs at the cell membrane surfaces would trigger the similar resealing process to make cells repair themselves. To answer this question by using convincing experimental results would also help to find an optimum acoustic pressure amplitude range achieving best delivery-efficiency and minimize possible side-effects in future clinical applications such as the targeting drug delivery.

The main goal of this study is to further understand the mechanisms of the reparable sonoporation. It is hypothesized that protein content in a plasma membrane of a cell which experiences reparable sonoporation caused by nearby oscillating EMBs under US excitation would increase as a consequence of the self-resealing action described above. Furthermore, it is hypothesized that there should be an optimum acoustic pressure amplitude range *in situ* that would generate most effective reparable sonoporation, below which no sonoporation effect would be observed and above which the disruption generated by sonoporation would be too severe to be repaired.

* Corresponding author. Tel.: +86 25 83792576; fax: +86 25 83272460.
E-mail address: guning@seu.edu.cn (N. Gu).

0168-3659/$ – see front matter © 2008 Elsevier B.V. All rights reserved.
doi:10.1016/j.jconrel.2008.07.038

2. Materials and methods

2.1. The preparation of NBD-labeled microbubbles

1, 2-Dipalmitoyl-*sn*-glycero-3-phosphoethanolamine-*N*-[methoxy (polyethylene glycol)-2000] (ammonium salt) (DPPE-PEG2k) and 25-{*N*-[(7-nitro-2-1, 3-benzoxadiazol-4-yl)-methyl] amino}-27-norcholesterol (25-NBD-cholesterol) were purchased from Avanti Polar Lipids, Inc. (Alabaster, AL). The L-α-phosphatidylcholine(PC, lyophilized powder) was purchased from Sigma-Aldrich, Inc. N_2 and all other reagents were analytical grade and were used as received.

PC/DPPE-PEG2k/25-NBD-cholesterol (90:5:5, molar ratio) dissolved in chloroform were added to the round bottom flask. Chloroform was removed under a vacuum evaporation until the thin film formed. A phosphate buffer solution (PBS, pH=7.4±0.1) was added to the dried lipids thin films to create a lipid concentration of 1 mg/ml. Then the lipid suspension was well mixed above the phase transition temperature of the lipids (60 °C) to form a milky solution of multi-lamellar liposomes with 25-NBD-cholesterol incorporated into the lipid membrane. Then the multi-lamellar liposomes suspension was continuously sonicated at 100 W with a probe while constant purging using a steady (4 ml/min) stream of N_2 gas for 5 min to form the microbubbbles. After centrifugal separation at 1500 rpm for 5 min (Eppendorf centrifuge 5804R, Brinkmann Instruments, Wesbury, NY, USA), the diameter of microbubbles was measured using Mastersizer 2000 (Malvern, England). Microbubbles for immunofluorescence experiment, the composition is PC/DPPE-PEG2k/cholesterol (90:5:5, molar ratio).

2.2. Cell culture and pretreatment

MCF7 (a human breast cancer cell line) cells, were cultured as monolayers in RPMI1640 media and 10% fetal bovine serum (FBS). They were grown in a humidified 5% CO_2 atmosphere at 37 °C. For US exposure experiments, exponentially growing cells were harvested and resuspended in fresh RPMI 1640 media with 10% FBS. The concentration of the cells was diluted to a concentration of ~10^6 cells/ml and mixed with the NBD-labeled microbubbles solution of the same concentration. For each trial, 1 ml cells suspension and 0.5 ml microbubbles solution were placed into a plastic tube of 15 mm diameter and 75 mm length (Kimble, Owens-Illinois, Toledo, OH).

2.3. Ultrasound apparatus and the ultrasound exposure

The ultrasound exposure system was shown in Fig. 1. An arbitrary waveform generator (Agilent 33250A, USA) was used to produce a sinusoidal radio frequency signal; it contained repeated 1 MHz tone-bursts, 20 cycles per tone-burst at a pulse repetition frequency (PRF) of 10 kHz. It was then amplified by a 50 dB broadband RF power amplifier (ENI 2100L, Rochester, NY, USA), and used to drive a self-made focusing transducer of radius 9.2 cm. The central frequency of the transducer is 1 MHz and the focal distance was 8 cm. The plastic test tube of 15 mm diameter and 75 mm length filled with cell and microbubble suspension capped by a rubber stopper (a rubber stopper was used as an sound absorber to minimize a standing-wave effect; there was no air between the cap and suspension) was rotated at 60 rpm by a DC motor throughout the exposure period; the rotation helped to mix microbubbles with cells evenly.

The transducer and test tube were immersed and mounted in a glass tank filled with de-ionized and degassed water. The test tube was aligned axially with the transducer in such a way that the center of the cell-suspension in a test tube was situated at an 8 cm distance from the surface of the source transducer.

A calibrated needle broadband hydrophone (TNU0001A, NTR, Seattle, WA, USA) with an active diameter of 0.6 mm and an upper frequency limit of 20 MHz and a low-noise 30 dB preamplifier (HPA30, NTR, Seattle, WA, USA) were used to measure the acoustic pressure *in situ*. The calibration of hydrophone was done using the combination of the beam scan-integration technique and the acoustic power measurement using the acoustic irradiation force [25]. The attenuation of the wall of test tubes was found by measuring the ultrasound amplitude with/without placing the test tube *in situ* and before the hydrophone using a short US tone-burst. The *in situ* spatial peak-pressure amplitude after attenuation correction, p_{sp}, changed with applied voltage to the power amplifier. In the experiment, output of the function generator was adjusted ranging from 400 mV to 1000 mV with a 200 mV increment, corresponding to 400 mV, 600 mV, 800 mV and 1000 mV voltage, the respective acoustic pressures amplitudes, p_{sp}, were 0.19, 0.25, 0.38, 0.48 MPa as measured by using the calibrated hydrophone. The total exposure time was 40 s.

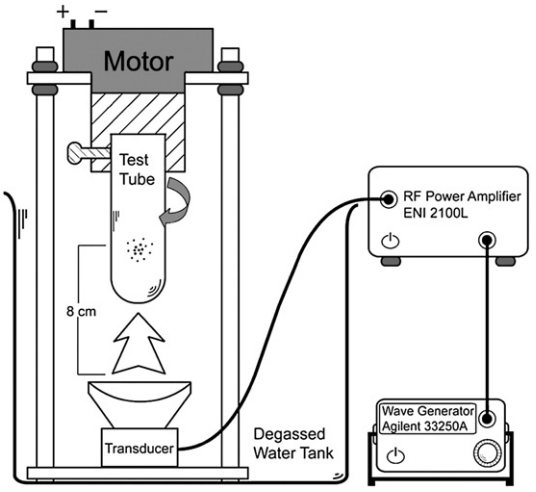

Fig. 1. The schematic diagram of ultrasound exposure apparatus. A focusing transducer (radius=9.2 mm and focal length=8 mm) of 1 MHz was used.

2.4. Characterization of cell morphology after the ultrasound exposure

2.4.1. Fluorescent microscopy

The optical observations and imaging were achieved by using the epifluorescent mode (excitation wavelength 440 nm, fluorescence wavelength 530 nm) of a microscope equipped with a digital Coolsnap MP3.3 camera (Axioskop 200, Carl Zeiss, Germany). The samples were imaged in real time immediately after sonication.

2.4.2. Scanning electron microscopy (SEM)

To observe the effects of ultrasound exposure on cell membranes, MCF7 breast cancer cells for each case were imaged using the scanning electron microscopy (SEM) at the different magnification. After ultrasound exposure, each sample was fixed with 2.5% glutaraldehyde solution for 1 h at −4 °C and then washed twice in 0.1M phosphate buffered saline (PBS, pH=7.2±0.1). Alcohol dehydration was followed in 33%, 50%, 66%, 80%, 90% and 100% ethanol for 20 min respectively, each stage being repeated twice. Then critical point drying was performed using Critical Point Driers (Emitech K850X, UK), after which the samples were gold sputter-coated for 5 min at 125 mA in an argon atmosphere with the approximately 50 nm coating (Emitech K550X Sputter Coating Systems, England). A field emission scanning electron microscope (SEM, FEI Sirion-200, USA) was used with a gun acceleration voltage of 20.0 kV and a working distance of 8 mm. The secondary electron detector was used to image the samples condition.

2.4.3. Flow cytometry assay

After the US exposure, the cells were separated from NBD-labeled microbubbles in suspension by centrifugation (1000 rpm, 8 min, Eppendorf centrifuge 5804R, Brinkmann Instruments, Wesbury, NY,

USA) and washed twice with phosphate buffer solution (PBS, pH=7.4±0.1) at room temperature and the cells were resuspended in PBS and then run by a BD FACSCalibur flow cytometer using CellQuest Pro software (BD Biosciences, Franklin Lakes, NJ, USA). The NBD fluorophore was detected and analyzed with an argon laser (excitation wavelength=488 nm, equipped with a 530 nm/30 nm bandpass filter for detection). The flow cytometry assay of the samples was performed in triplicate and reported as mean±standard deviation.

2.5. Protein determination

The protein contents in cell supernatant were measured using the Bradford assay after separating the cells. The Bradford assay can be finished in 5–15 min and has sensitivity of 1–5 μg for determining protein content of cell fractions (instruction booklet, Bio-Rad Corporation). The assay is based on the observation that the absorbance maximum for an acidic solution of Coomassie Brilliant Blue G-250 shifts from 465 nm to 595 nm when binding to protein occurs. The relative protein concentrations were determined following the instruction provided by Bio-Rad Corporation using bovine serum albumin as the standard and Bradford reagents consisting of Coomassie Brilliant Blue G-250 and phosphoric acid. The total protein contents of extraction solution were analyzed.

2.6. LAMP-1 immunofluorescence studies

2.6.1. Optical microscopy

Phycoerythrin (PE) anti-mouse CD107a (PE-LAMP-1) was purchased from eBioscience, Inc. To investigate the involvement of lysosomal exocytosis in plasma membrane repair, the luminal domain of LAMP-1 on the surface of MCF7 cells was examined prior-and post-US exposure. The samples immediately after 0, 0.19, 0.25, 0.38, 0.48 MPa US exposure were separately spun on pre-treated poly-L-lysinecoated coverslips (30 mm×30 mm) by a cytospin of cell-centrifugation-smear machine (Statspin Cytofuge2, IRIS, USA) at 1200 rpm for 5 min. Then samples on coverslips were fixed for 90 min at room temperature in 4% paraformaldehyde solution. After that, the samples on coverslips were washed in PBS(pH=7.4±0.1) triplicate and immunostained using standard protocols with PE-LAMP-1 antibody solution for 1 h at 37 °C under humidified chamber. After staining, cells in samples were washed four times with cold PBS and were sealed with 50% glycerol to observe under the fluorescent microscope.

2.6.2. Flow cytometry

Cells were fixed for 90 min at room temperature in 4% paraformaldehyde for a few seconds after US exposure. PE-LAMP-1 immunofluorescence staining in the cell solution was then treated using a standard protocol, and was analyzed using BD FACSCalibur flow cytometer. The fluorophore of PE red marker compounds was measured with a 488 nm argon laser excitation and a 575 bandpass filter for emissions. The whole amount of cell surface uptake level was quantified by converting to an average number of molecules per cell. At the same condition, the flow cytometry assay of the samples was measured in triplicate and the average results were presented.

3. Results

3.1. The concentration and size of the microbubbles

The mean diameter of NBD-labeled microbubbles was measured to be (1.156±0.19) μm (mean±standard deviation for $n=3$) for a distribution with polydisperity index (PI) of 0.11 using the laser particle sizer Mastersizer 2000. The number of lipid microbubbles created from 1 mg total lipid with the composition used in the experiment was estimated to be 1.1×10^{11}/ml. Before microbubbles were used in the study, the solution was diluted by the PBS to the concentration of $2–6\times10^{6}$ microbubbles/ml, which was measured and confirmed by the laser particle sizer Mastersizer 2000 after it was diluted.

After sonication, the decrease of both the concentration and the mean size of the microbubbles were observed using an optical microscope. This was further confirmed by an experiment performed on microbubble suspension without cells. After sonication under 0.19 MPa, 0.25 MPa, 0.38 MPa and 0.48 MPa, the mean diameters decreased to be 809.38±80.4 nm, 785.71±71.4 nm, 533.33±34.3 nm and 357.14±24.1 nm respectively; the concentrations also changed to 5.8×10^{4}, 3.3×10^{4}, 2.4×10^{3} and 6.0×10^{2} microbubbles per ml respectively.

3.2. The fluorescent efficacy of NBD fluorophore

After US exposure, the sample was isolated and washed by centrifugation flotation allowing observations by the optical microscopy and a flow cytometry. Fig. 2(A) shows a fluorescent image of the microbubbles under a 40× lens before the ultrasound exposures. Fig. 2(B) and (C) contain images of MCF7 cells without US exposure under the bright field and epifluorescent field respectively. Fig. 2(D) and (E) include bright field and fluorescence images of the cells exposed to US irradiations. The images show that the NBD fluorophore could be fused with the plasma membrane or be delivered inside of the cells upon sonication and then the cell self-resealing made the cells viable.

3.3. Morphology of MCF7 cells

Fig. 3 shows the SEM images (the magnification=5000) of cells under different p_{sp} US exposures. Normally the morphology of the MCF7 cells

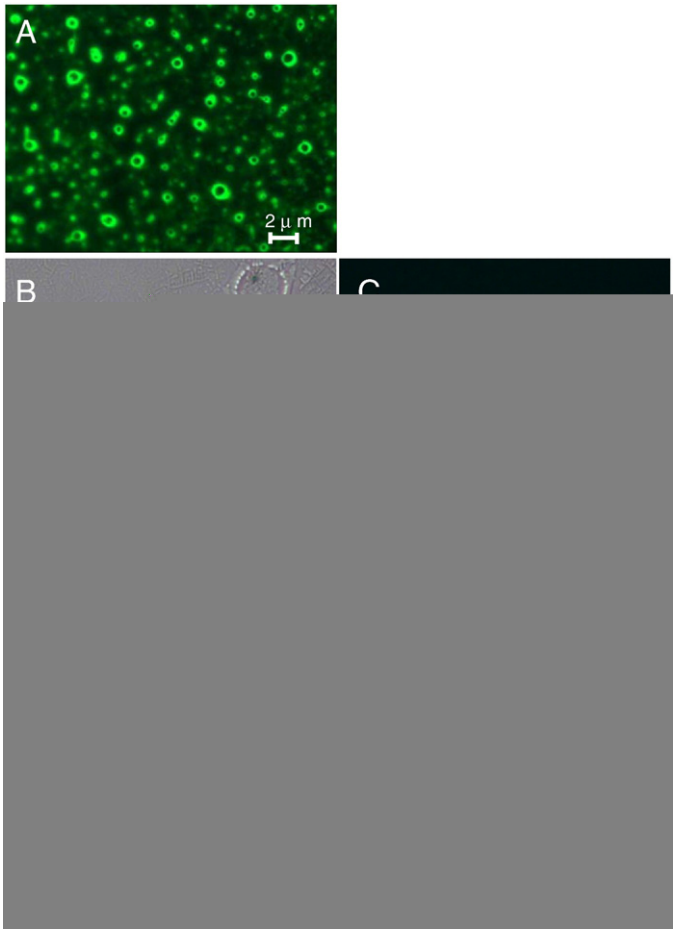

Fig. 2. Fluorescent images of NBD-labeled lipid-encapsulated microbubbles (A) (40×); B and C were images of cells without ultrasound exposure under the bright field and fluorescent field (20×); D and E were images of cells in the presence of microbubbles after p_{sp}=0.25 MPa ultrasound exposure for 40 s under the bright field and fluorescent field (20×) respectively.

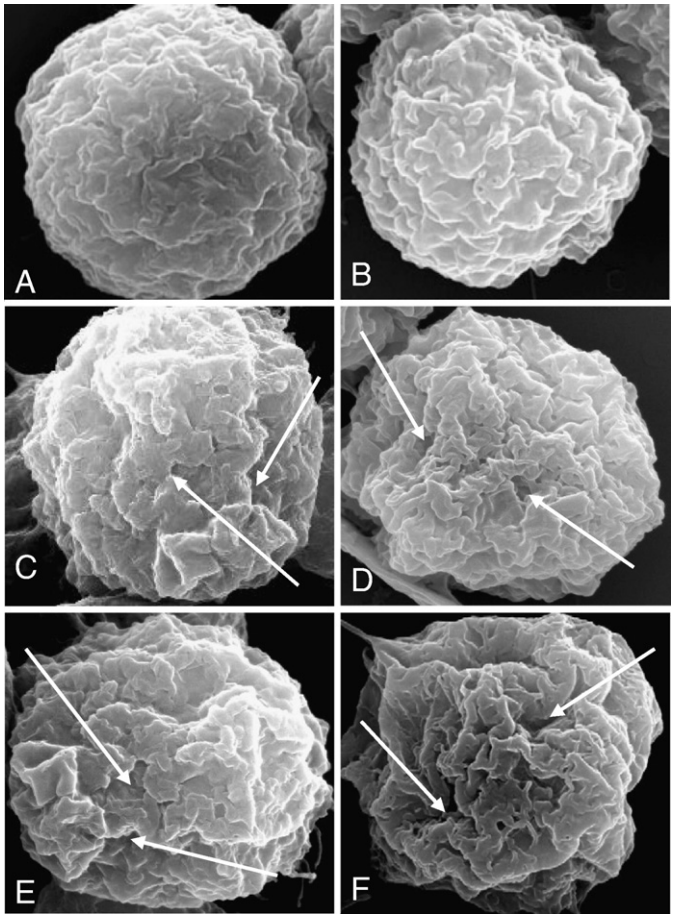

Fig. 3. Scanning electron microscopic images of MCF7 cells irradiated with ultrasound in the presence of EMBs. No US (A), US but no EMBs presence (B). After p_{sp}=0.19, 0.25, 0.38 and 0.48 MPa exposure for 40 s with EMBs presence, respectively (C to F).

is of spherical shape and their surfaces are relatively smooth (Fig. 3A). Dimple-like craters of various sizes appeared in the membrane surfaces in many cells after US exposures with EMBs' presences during our experiment. Fig. 3B is an image of a MCF7 cell obtained after the US treatment (acoustic pressure amplitude p_{sp}=0.25 MPa) without EBMs' presence. No pores were observable. Fig. 3C to F are images corresponding to p_{sp}=0.19 MPa, 0.25 MPa, 0.38 MPa, 0.48 MPa respectively with EMBs' presence. The size of the pores were estimated to be in the range 1 nm–94.3 nm, 10 nm–533 nm, 786 nm–1.11 μm and 2.03 μm–4.31 μm respectively. Rough regions and small pits started to reveal when acoustic pressure amplitude increased as shown in Fig. 3C–E. It is interesting to note that although the same p_{sp} (0.25 MPa) was used in tests, Fig. 3(B) looks different from Fig. 3(D); the presence of oscillating EMBs (Fig. 3 D) near cells introduced a few pits at the cell membrane. This difference in cell surface morphology indicates US effects on cells were amplified by the EMBs. It is noted that the 'holes' in Fig. 3(F) are conspicuously 'large'. It suggests that the hole size might have reached the level beyond repairing via self-sealing mechanism, i.e., non-reparable sonoporation (sonolysis) might take place [5].

Table 1
Summary of sonoporation efficiency

Spatial peak				
Acoustic Pressure Amplitude	0.19 MPa	0.25 MPa	0.38 MPa	0.48 MPa
Efficiency (%)	1.88	15.63	10.75	8.78

3.4. The NBD fluorophore flow cytometry results

The percent fluorescence intensity increases relative to a control case (cells were not sonicated) measured by the flow cytometry is defined as the sonoporation efficiency for the comparison purpose. Fig. 4 is a plot of the mean fluorescence intensity (n=3) *vs* p_{sp}. The mean fluorescence intensity as shown in Fig. 4 initially increases as p_{sp} increases and reaches the maximum when p_{sp}=0.25 MP and then decreases. Table 1 summarizes the sonoporation efficiency of different p_{sp} .

3.5. Quantification of protein content

Fig. 5 shows the averaged whole protein content per 1 ml supernatant of the cells post the US exposures. The protein content in the supernatant

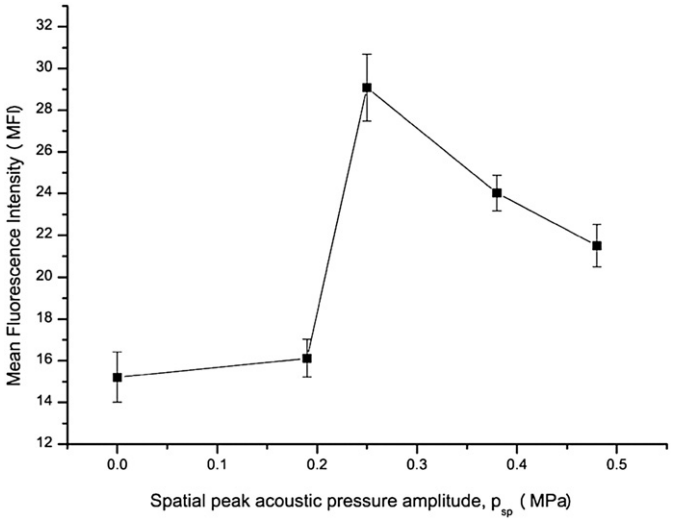

Fig. 4. Flow cytometric analysis of MCF7 cells absorbing the NBD fluorescence on the surface or into the plasma. The histogram shows that there is different absorbing efficiency under different ultrasound voltage exposure. The case of p_{sp}=0.25 MPa yielded the maximum mean fluorescence intensity. Each data point represents the average of triplicate measurements and the error bars are the standard deviations (SD) of the triplicate measurements.

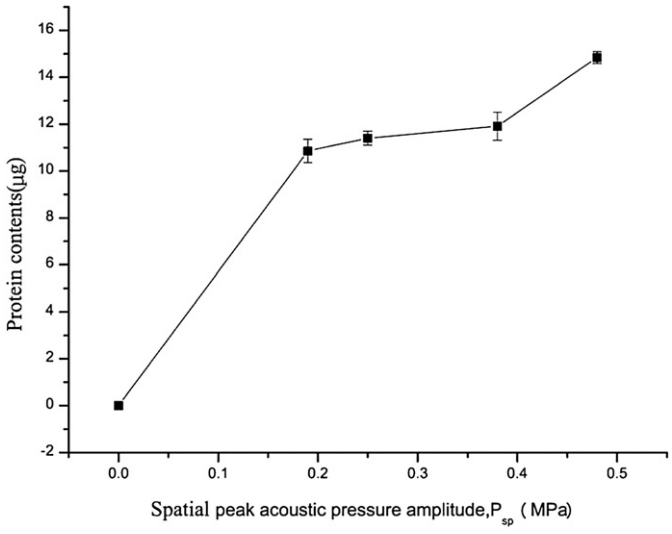

Fig. 5. The protein concentrations in supernatant after separating the cells under different US exposures. The protein contents in supernatant have significantly increased after sonoporation. At p_{sp}=0.48 MPa, the extra amounts of proteins might came from the leakage due to bigger pores on the membrane surface. Each data point represents the average of triplicate measurements and the error bars are the standard deviations (SD) of the triplicate measurements.

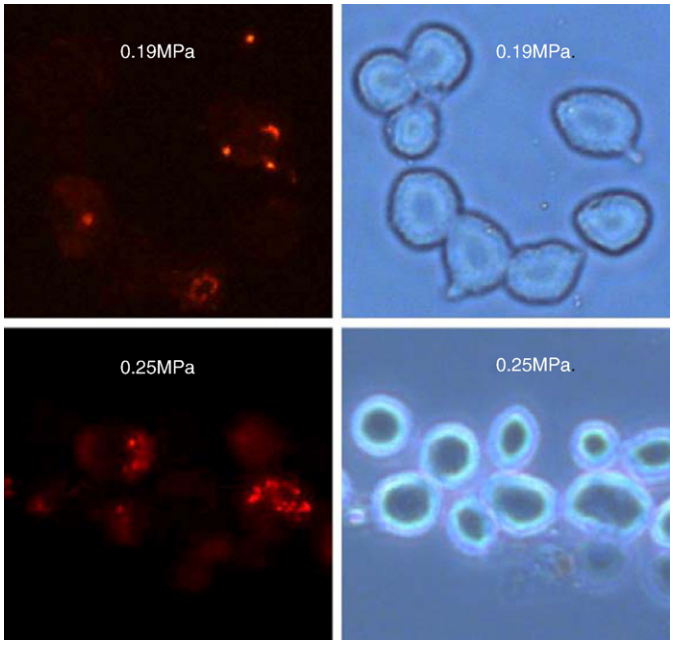

Fig. 6. Staining of a resealed MCF7 cells after US exposure (p_{sp}=0.19 and 0.25 MPa) with antibodies against a luminal domain of the lyososome-specific protein, LAMP-1. Surface exposure of LAMP-1, indicated by the staining, is evident over the resealed disruption site. This provides strong evidence that the local exocytotic response evoked by a disruption utilizes lysosomes.

(PCS) increases significantly when p_{sp} increases from 0 (control) to 0.19 MPa. Between 0.19 and 0.38 MPa, PCS increases slightly and the increase-rate (slope) of PCS becomes much greater when p_{sp}>0.38 MPa.

3.6. LAMP-1 exposure on the cell surface after sonoporation

The results of PE-LAMP-1 staining with antibodies against a luminal domain of the lyososome-specific protein are shown in Fig. 6. LAMP-1 did not stain the surface when p_{sp}=0, 0.38 and 0.48 MPa. When p_{sp}=0.19 and 0.25 MPa, LAMP-1 were strongly stained on the surface of cells.

Results of the flow cytometric PE fluorophore analysis obtained by the LAMP-1 specific immunofluorescence staining show that the adsorption capacities are 21.02± 3.51%, 22.57± 5.26% for p_{sp}=0.19 and 0.25 MPa and 0% for p_{sp}=0.38 and 0.48 MPa US exposure respectively (n=4).

4. Discussion

4.1. Spatial peak acoustic pressure amplitude, p_{sp}, determines sonoporation efficiency

The sonoporation efficiency of MCF7 cells as defined above was determined by the flowcytometry assay as shown in Table 1. The values of p_{sp} were chosen to see whether the mean fluorescent intensity had a trend to reach a maximum. It has been unequivocally demonstrated that the trend does exist and application of p_{sp}=0.25 MPa had the highest efficiency among all acoustic pressure amplitudes we tested. The SEM images in Fig. 3 also show that the surface morphology of the cell membrane of the p_{sp}=0.25 MPa case although it was compromised somewhat by sonoporation but still maintained a good surface condition; i.e., the cell membranes repaired themselves via self-sealing as suggested by Fig. 6. It seems to support the above conclusion that a moderate US field in the neighborhood of p_{sp}=0.25 MPa is the optimum acoustic pressure amplitude for high sonoporation efficiency in all values of p_{sp} applied. During sonication, the oscillation-amplitude of EMBs might be relatively small and stable; i.e. non-inertial cavitation was involved [10]. If p_{sp} became much greater than 0.25 MPa, EMBs might undergo very rigorous nonlinear oscillation; inertial or transient cavitation might take place. It is possible that the dramatic nonlinear oscillations of the EMBs might render the cells permanently deformed. If it happens, this process is non-reversible and very often produces cell lysis. Fig. 3(F) indicates that large rough areas with folds and "holes" appear at the membrane surface of a cell after sonication at p_{sp}=0.48 MPa. Data of Figs. 4 and 5 also suggest at p_{sp}=0.48 MPa MFI was low and protein content was high; the latter might be caused by the leakage of the cytoplasmic material through cell membranes. The dramatic decreases of bubbles' concentration and mean size also support the idea that for high p_{sp} the bubble oscillations may be destructive.

4.2. The possible mechanism of cell resealing

Sonoporation-induced exocytosis of lysosomes and plasma membrane resealing under the optimum ultrasound exposure have been observed in our study. In the experiment of the uptake of fluorophor into the MCF7 breast cancer cells after ultrasound exposure, the maximum peak of fluorescent absorption was found at p_{sp}=0.25 MPa US radiation. Further increase of p_{sp}, the adsorption decreased. Fig. 6 shows that anti-LAMP-1 did not stain the surface when p_{sp}=0.38 and 0.48 MPa, but strongly stained the surface when p_{sp}=0.19, 0.25 MPa.

Our experiment also suggested that it is likely that the resealing process occurred during the reparable sonoporation (p_{sp}=0.19, 0.25 MPa); i.e., cell membrane disruption generated by shear stress due to oscillating EMBs excited by US might trigger Ca^{2+} entering the disruption area and cause vesicles to present in cytoplasm underlying the disruption site to fuse rapidly with one another and also with the adjacent plasma membrane. Consequently, LAMP-1 protein became exposed at the plasma membrane surface.

5. Conclusions

This experiment has demonstrated that moderate US (p_{sp}=0.25 MP, repeated 1 MHz tone-bursts, 20 cycles per tone-burst at PRF of 10 kHz) exposures up to 40 s assisted by the presence of EMBs caused reparable sonoporation of MCF7 human breast cancer cells to occur. It was also demonstrated that US induced shear stress at the cell membranes generated small pores by which cells could uptake some of its extracellular fluid. The pores were repaired through the self-sealing in a few seconds. Our findings may play an essential role in the target-drug delivery applications. In such applications, the choice of adequate acoustic pressure amplitude is important. If p_{sp} is too small, sonoporation will not be induced. If p_{sp} is too great, non-reparable sonoporation may be induced; the disruption of cell membranes can be too great to be repaired by self-sealing.

Acknowledgments

This investigation was partially funded by the National Important Science Research Program of China (Nos. 2006CB933206) and National Natural Science Foundation of China (Nos. 60371027, 60171005, 90406023). Fang Yang is also thankful for the Scientific Research Foundation of Graduate School of Southeast University. We wish to extend our appreciation to professor Fan Li for the kind help of the scanning electron microscopy experiments.

References

[1] S. Bao, B.D. Thrall, D.L. Miller, Transfection of a reporter plasmid into cultured cells by sonoporation *in vitro*, Ultrasound Med. Biol. 23 (1997) 953–959.
[2] D.L. Miller, S. Bao, J.E. Morris, Sonoporation of cultured cells in the rotating tube exposure system, Ultrasound Med. Biol. 25 (1999) 143–149.
[3] D.L. Miller, J. Quddus, Lysis and sonoporation of epidermoid and phagocytic monolayer cells by diagnostic ultrasound activation of contrast agent gas bodies, Ultrasound Med. Biol. 27 (2001) 1107–1113.

[4] D.L. Miller, C. Dou, J. Song, DNA transfer and cell killing in epidermoid cells by diagnostic ultrasound activation of contrast agent gas bodies *in vitro*, Ultrasound Med. Biol. 29 (2003) 601–607.
[5] M. Ward, J. Wu, J.F. Chiu, Ultrasound-induced cell lysis and sonoporation enhanced by contrast agents, J. Acoust. Soc. Am. 105 (1999) 2951–2957.
[6] M. Ward, J. Wu, J.F. Chiu, Experimental study of the effects of Optison concentration on sonoporation *in vitro*, Ultrasound Med. Biol. 26 (2000) 1169–1175.
[7] J. Wu, Theoretical study on shear stress generated by microstreaming surrounding contrast agents attached to living cells, Ultrasound Med. Biol. 28 (2002) 125–129.
[8] J. Wu, J. Pepe, M. Ricon, Sonoporation, anticancer drug and antibody delivery using Ultrasound, Ultrasonics 44 (2006) e21–e25.
[9] J. Wu, D. Chen, J. Pepe, B.E. Himberg, M. Ricón, Application of liposomes to sonoporation, Ultrasound Med. Biol. 32 (2006) 429–437.
[10] J. Wu, W. Nyborg, Ultrasound, cavitation bubbles and their interaction with cells, Adv. Drug Deliv. Rev. 60 (2008) 1103–1116.
[11] J. Wu, Sonoporation, gene transfection, anticancer drug and antibody drug delivery in emerging therapeutic ultrasound, in: J. Wu, W.L. Nyborg (Eds.), World Scientific Co., Hackensack, New Jersey, USA, 2007, pp. 219–246.
[12] W.J. Greenleaf, M.E. Bolander, G. Sarkar, M.B. Goldring, J.F. Greemleaf, Artificial cavitation nuclei significantly enhance acoustically induced cell transfection, Ultrasound Med. Biol. 24 (1998) 587–595.
[13] A. Lawrie, A.F. Brisken, S.E. Francis, Microbubble-enhanced ultrasound for vascular gene delivery, Gene Ther. 7 (2000) 2023–2027.
[14] A. Wamel, K. Kooima, M. Harteveld, M. Emmer, F.J. Cate, M. Versluis, N. Jong, Vibrating microbubbles poking individual cells: drug transfer into cells via sonoporation, J. Control. Release 112 (2006) 149–155.
[15] D.M. Hallow, A.D. Mahajan, M.R. Prausnitz, Ultrasonically targeted delivery into endothelial and smooth muscle cells in *ex vivo* arteries, J. Control. Release 118 (2007) 285–293.
[16] M.D. Eshet, D. Adam, M. Machluf, The effects of albumin-coated microbubbles in DNA delivery mediated by therapeutic ultrasound, J. Control. Release 112 (2006) 156–166.
[17] J. Wu, Shear stress in cells generated by ultrasound, Prog. Biophys. Mol. Biol. 93 (2007) 363–373.
[18] P. Prentice, A. Cuschieri, K. Dholakia, M. Prausnitz, P. Campbell, Membrane disruption by optically controlled microbubble cavitation, Nat. Phys. 1 (2005) 107–110.
[19] G.A. Husseini, W.G. Pitt, Miscelles and nanoparticles for ultrasonic drug and gene delivery, Adv. Drug Deliv. Rev. 60 (2008) 1137–1152.
[20] T.A. Tran, S. Roger, J.Y. Le Guennec, F. Tranquart, A. Bouakaz, Mechamisms of cell membrane permeabilization with ultrasound and contrast microbubbles, IEEE Ultrason. Symp. (2005) 5–8.
[21] A. Reddy, E.V. Caler, N.W. Andrews, Plasma membrane repair is mediated by Ca^{2+}-regulated exocytosis of lysosomes, Cell 106 (2001) 157–169.
[22] P.L. McNeil, Repairing a torn cell surface: make way, lysosomes to the rescue, J. Cell Sci. 115 (2002) 873–879.
[23] P.L. McNeil, T. Kirchhausen, An emergency response team for membrane repair, Nat. Rev., Mol. Cell Biol. 6 (6) (2005) 499–505.
[24] R.E. Kumon, P. Parikh, D. Sabens, M. Aehle, D. Kourennyi, C.X. Deng, Ultrasound-induced calcium oscillations and waves in Chinese hamster ovary cells in the presence of microbubbles, Biophys. J. 93 (6) (2007) L29–31.
[25] K. Beissner, M.C. Ziskin, P.A. Lewin (Eds.), Measurement techniques ultrasonic exposimetry, CRC Press, Boca Raton, Florida, USA, 1993, pp. 127–142.